

Fast LLM Post-training via Decoupled and Best-of-N Speculation

Rongxin Cheng^{1,2}, Kai Zhou², Xingda Wei^{*1}, Siyuan Liu¹, Mingcong Han^{1,2}, Mingjing Ai³, Yeju Zhou², Baoquan Zhong², Wencong Xiao², Rong Chen¹, and Haibo Chen¹

¹Institute of Parallel and Distributed Systems, Shanghai Jiao Tong University

²ByteDance Seed

³Unaffiliated

Abstract

Rollout dominates the training time in large language model (LLM) post-training, where the trained model is used to generate tokens given a batch of prompts. SPECACTOR achieves fast rollout with speculative decoding that deploys a fast path (e.g., a smaller model) to accelerate the unparallelizable generation, while the correctness is guaranteed by fast parallel verification of the outputs with the original model. SPECACTOR addresses two foundational challenges in speculative rollout by (1) a *dynamic decoupled speculation* execution method that maximizes the GPU computational efficiency to realize speedup for large-batch execution—a configuration common in training but unfriendly to speculative execution and (2) a *dynamic Best-of-N speculation* method that selects and combines different drafting methods according to the rollout progress. It substantially improves the speculation accuracy even when the best drafting method is unknown *a priori*, meanwhile without requiring adding extra computation resources. SPECACTOR is 1.3–1.7 \times faster than common post-training baselines, and is 1.3–1.5 \times faster compared to naively adopting speculative decoding for rollout.

1 Introduction

Large Foundational Models like LLMs have demonstrated remarkable accuracy across a wide range of tasks including but not limited to writing [40], coding [42], and many others [38]. Post-training these models with reinforcement learning (RL) has become a key pillar in the training pipeline to further unleash LLM capabilities in challenging tasks such as reasoning [10].

Rollout is a key and performance-dominant phase in post-training (§2.2): at each step, the system feeds the model with a batch of prompts representing target problems (e.g., math or coding problems) for LLMs to solve. The model then generates tokens for each prompt attempting to solve them. When rollout finishes, the generated tokens are evaluated and the model is updated accordingly. Rollout is naturally parallelized across multiple workers.

Problem statement and current solutions (§2.2).

Rollout

suffers from lengthy execution issues (accounting for up to 80 % of the training time), due to long tails in generation time, which is further exacerbated by idle GPU time (see Figure 2) caused by waiting for the slowest worker to finish. The long tail stems from difficulty variation, with some problems requiring more tokens than others to solve. Therefore, one worker may finish its assigned prompts quickly, while another takes much longer to complete. Waiting for all requests to update the model is necessary to ensure rapid training convergence from an algorithm perspective [43, 45, 61].

We tackle a specific but important question: *how to accelerate rollout in LLM post-training without changing how the model is trained?*

Existing algorithm-agnostic solutions fall into two categories, neither of which adequately addresses the issue—especially for long-tail generation, which is increasingly common as LLMs tackle more challenging problems [20, 33]. The first category is *overlapping*, which utilizes idle worker GPUs to execute other post-training phases [70] and overlaps different phases to reduce idle time. However, overlapping does not directly accelerate the rollout—it only improves other phases. In long-tail generation, where rollout dominates the training time, its speedup is limited (1.1 \times on average). The second category accelerates rollout by leveraging *parallelism*. For example, a recent work RLBoost [6] dynamically spawns more GPUs for rollout. Unfortunately, we found that adding more GPUs provides limited speedup (e.g., up to 1.2 \times) because (1) LLM rollout generates tokens sequentially, and (2) generating one token is memory-bound, so additional computational power helps little. Moreover, deploying more GPUs results in a smaller batch size per worker, which is impractical in real-world scenarios due to low GPU utilization and limited training budget (see Figure 6 (a)).

Our work: speculative rollout. We present SPECACTOR, a fast rollout system that retrofits speculative decoding—a common technique for accelerating LLM inference—to LLM post-training. At a high level, speculative decoding employs a fast draft path for sequential generation, i.e., generation with a small model. First, a small “draft” model generates a sequence of draft tokens (e.g., 3). Then, the trained model verifies these tokens. Once accepted, these tokens are treated

^{*}Xingda Wei is the corresponding author (wxdwfc@sjtu.edu.cn).

as generated by the trained model. The rationale is that verification is typically faster than generation—although both verification and generation use the same model—because verification processes multiple tokens in parallel, while generation is sequential. It is important to note that speculative decoding can preserve the exact same generation results as the trained model with exact matching [57].

While intuitive, naively applying speculative decoding to rollout (e.g., following the method in RhymeRL [16]) yields only 10–20 % rollout speedup in our evaluation in §5.3. Two fundamental obstacles limit its effectiveness and we address them with the following two contributions.

Efficient speculative rollout on large batches with dynamic decoupled speculation (§4.1). Speculative decoding provides little speedup for large batches—a limitation also noted by recent work [27, 32]. We found that large batch sizes (e.g., 128) are common in post-training, and although the batch size decreases during rollout, it remains large (i.e., ≥ 64) for 20 % rollout time (see §3). The limited speedup occurs because verification has much higher computational intensity than decoding. As a result, a large batch can quickly reach the GPU computational bound, making verification slower than generation.

We propose dynamic decoupled speculative execution, a new speculative decoding execution paradigm that significantly improves execution efficiency in large batches. Decoupling means relaxing the draft-verification barrier in existing algorithms such that we can fully disaggregate drafting and verification to allocate more GPU time to the computation-intensive verification. Thanks to the improved computational efficiency, decoupled execution quickly shrinks the per-worker batch size during rollout. However, we still face the challenge of decreased verification acceptance rate, because relaxing the barrier comes at the cost of extra waste due to unverified drafting. To this end, we further design a feedback mechanism such that we can dynamically control the degree of relaxing as well as leverage Best-of-N speculation (described next) to improve the acceptance rate.

Efficient approximating the best drafting method with dynamic Best-of-N speculation (§4.2). Speculative decoding struggles to mitigate long-tail generation. We found that the root cause is low acceptance rates due to improperly selected drafting methods. However, selecting the optimal drafting method is challenging for two reasons: (1) faster drafting methods (e.g., using smaller models) typically have lower acceptance rates, and (2) acceptance rates vary significantly across requests and cannot be known in advance. Running multiple drafting methods in parallel is also impractical as it requires extra GPUs.

Our Best-of-N speculation efficiently approximates the “best” drafting method for each request using the following three techniques. First, we propose a new abstraction called *draft ladder* that establishes a mapping from various accep-

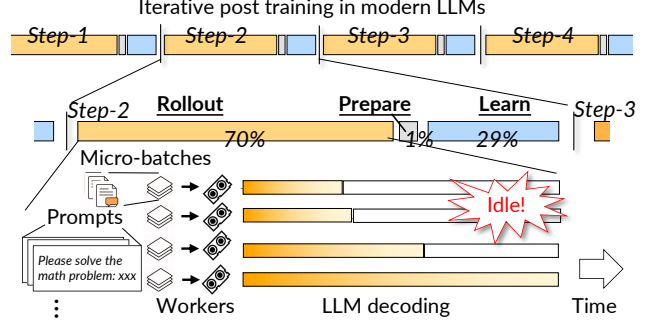


Figure 1: An illustration of the rollout process in LLM post-training.

tance rates to speedup given a pool of available drafting methods, which can be constructed offline. Given the ladder, at the beginning of rollout, we select one estimated best drafting method using the average acceptance rate profiled so far. The rationale is that even though each prompt’s acceptance rate varies significantly, the average acceptance rate over a (large) batch of requests is statistically stable [17]. Thus, the selected drafting method is likely to be close to the optimal for the batch. Finally, when the batch size decreases during rollout and the initial selection becomes suboptimal, we utilize the freed GPU resources to launch more drafting methods in parallel for long-tailed requests, and the request is considered finished when the first drafting method succeeds. This increases the likelihood of obtaining the best drafting method with unknown acceptance rates, while not using additional GPU resources.

Demonstration. We built SPECACTOR, a prototype system integrated with popular post-training framework veRL [46] with efficient speculative decoding for rollout. We evaluated SPECACTOR with various real-world training traces. Compared to the state-of-the-art solutions like veRL, RLHFuse, SPECACTOR reduces the end-to-end training time by up to 40 %, and is up to 1.5 \times (from 1.3 \times) faster than naive speculative decoding methods utilized by a recent work [16].

2 Background and Motivation

2.1 Background on LLM post-training

Generation with LLM. Large Language Models (LLMs) generate responses (termed *tokens*) through *prefill* and *decode* phases. The prefill phase processes the initial input (termed *prompt*) to generate the first token. The decode phase then iteratively generates subsequent tokens in an auto-regressive fashion by combining previous output tokens with the original input as the new input. The decode phase terminates upon generating an end-of-sequence token.

Post-training workflow. Leading LLMs are post-trained with reinforcement learning (RL) with multiple steps of execution, where each step follows an identical three phases [10, 35, 71, 46]:

1. Rollout. The training treats the model as RL actors and generates tokens from a sampled batch of pre-defined prompts using the aforementioned LLM generation process. The tokens are used to solve specific tasks like math problems. To accelerate the rollout, the sampled batch is divided into smaller micro-batches (*batch*¹) such that the rollout can be concurrently executed across multiple *rollout workers*, where each worker holds a copy of the model parameters on one or multiple GPUs (in case one GPU has insufficient memory to hold a complete copy of the model parameters as well as the intermediate results) and processes a micro-batch of prompts (see Figure 1).

Two aspects need to be noted regarding the formulation of the rollout batch. First, to accelerate learning, production RL processes apply a relatively large rollout batch size to find positive rewards [22, 45, 60, 61, 68], e.g., a typical 32 B task sets the total batch size to 8 K [61, 62]. Second, each data point is typically seen a few times during the entire training process, i.e., most training involves only 1–2 epochs [8], making statistics-based techniques like experience replay [28] less effective.

2. Prepare. In the prepare phase, the rollout results are fed into a set of judges [45, 61, 63, 66] (e.g., a separate reward model) to generate rewards [43, 5], which are the arithmetic signals that guide the parameter optimization. These judges are lightweight; for example, the reward models only compute a forward pass, not a full LLM generation, so the time required is negligible in a rollout step.

3. Learn. Given the signals from the prepare phase, the learning phase calculates the loss and updates the LLM parameters with a backward pass. The updated parameters are then used in the next rollout step.

Training methodologies: on-policy vs. off-policy. On-policy training requires the rollout to process the batch using the latest learned model, i.e., there is a strict barrier between subsequent steps. For example, in Figure 1, step-2 must wait for the three phases in step-1 to finish to execute. In contrast, off-policy training [39, 11] allows the rollout to use older versions of the model, e.g., even if some prompts in step-1 have not finished the rollout, it uses the finished prompts to prepare and learn, and starts step-2 upon the learning. The unfinished prompts will be used in the next or future step upon their completion.

We focus on on-policy training for two reasons. First, on-policy training is most desirable for algorithm developers as it provides better guarantees on convergence and model quality theoretically [3, 41, 51]. Second, even though algorithm developers may choose off-policy training, they do not allow arbitrary delay of the learning of the unfinished prompts to ensure model quality [69, 11], so the overall behavior is similar to on-policy training. For example, a typical delay is set to

¹Since we only refer to micro-batches in the following content, we use the more general term *batch* to indicate micro-batch without loss of generality.

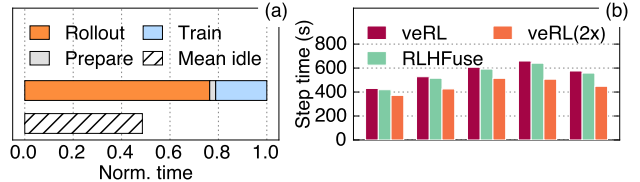


Figure 2: (a) The GPU idle problem in post-training and (b) the training latency of various steps in DAPO-32B-20K training trace (detailed setups described in §5.1).

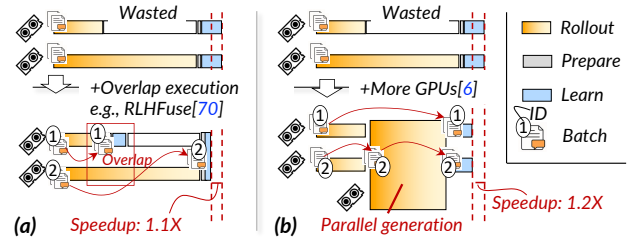


Figure 3: (a) An illustration of accelerating post-training via overlapped execution and (b) an illustration of accelerating rollout via dynamically adding more GPUs.

one, which means that the current unfinished rollout must be learned in the next step, so it may still suffer from long-tailed generation.

2.2 Analysis of post-training and current solutions

Rollout dominates execution time in post-training and suffers significant GPU wastes. Figure 2 (a) analyzes the contribution of total post-training time in typical training tasks: rollout contributes 70–80 % of the total training time. Since post-training could last for days on hundreds of thousands of GPUs, accelerating rollout is critical to reducing the overall training cost.

There exists significant space for improvement for rollout because many GPUs are idle during the rollout phase due to the long-generation tail problem. Figure 2 (a) shows the GPU bubble in long-tailed rollout: on a DAPO-32B-20K trace, we observed averagely 50 % of the total GPU time is wasted due to waiting for the slowest worker to finish. Rollout time differs significantly across workers—though they are assigned the same amount of tasks, the number of tokens required to solve different tasks varies significantly, and the exact number is hard to predict in advance as they are determined by the LLM outputs. Moreover, the waste increases as training progresses because as the model becomes smarter, it tends to generate more tokens to solve particular tasks [8]. In comparison, the prepare and learn phases exhibit minimal waste as their computation is relatively regular.

Reducing GPU waste via overlapping achieves a minor speedup for long-tail generation. An intuitive solution to reduce wasted GPU time is to overlap other phases with the current rollout: As shown in Figure 3 (a), representative solutions like RLHFuse [70] utilize the idle workers to ex-

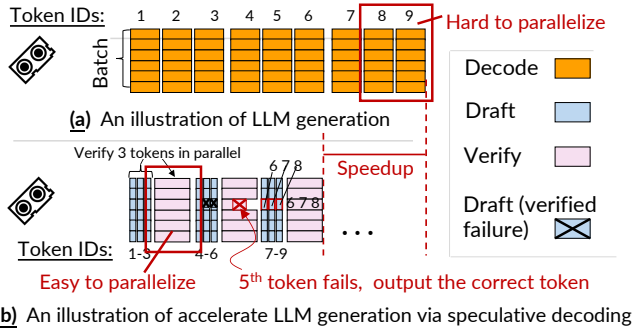


Figure 4: An illustration of using speculative decoding to accelerate LLM generation.

ecute the prepare and learn phases of finished batches (e.g., batch ①), overlapping these phases from fast workers with the rollout of slower workers. While such an overlap cannot accelerate the rollout phase—as it is bottlenecked by the slowest worker, it improves the end-to-end training time because once the slowest rollout finishes, more GPUs can participate in accelerating the prepare and learn phases of the slowest batch (e.g., batch ②).

However, the speedup from overlapping is limited because the accelerated prepare and learn phases only contribute a small portion of the overall training time (e.g., about 5% in Figure 2 (a)). As a result, RLHFuse only accelerates post-training by 3% in traces with long generation, GPU time still wasted, as shown in Figure 2 (b).

The sequential-generation nature of rollout is the key obstacle for accelerating rollout. Another intuitive solution is to dynamically add more computation resources to accelerate the long-tailed workers: as shown in Figure 3 (b), once a rollout worker finishes its assigned batch (e.g., batch ①), it can help accelerate the generation of unfinished batches (e.g., batch ②) using parallel LLM generation techniques like sequence parallelism [55]. Moreover, current works [6] aggressively add more GPUs (e.g., by allocating spot instances) to accelerate the slow rollout workers without waiting for more GPUs to become idle. In our example, three workers now process the rollout of batch ②. Unfortunately, as shown in Figure 2 (b), even if we provision $2 \times$ GPUs for rollout, the end-to-end training time is only improved by $1.2\text{--}1.3 \times$. The limited speedup is rooted from the sequential-generation and memory-bottlenecked nature of rollout: tokens need to be generated one-by-one, and generating one token is constrained by the memory that has limited room for parallelization due to the extra communication costs.

Current systems either suffer from limited speedup or adopt lossy acceleration methods like off-policy training or truncating tailed generations, as summarized in §7. We seek an algorithm-agnostic system solution for fast rollout.

3 Design Rationale and System Overview

Opportunity: speculative decoding for generation in rollout [7, 24, 27, 32, 49, 36]. It is a common technique for accelerating sequential LLM generation: As detailed in Figure 4 (a), the original generation iteratively generates tokens for the current batch, where each iteration is a forward execution of the trained model. With speculative decoding (b), we first generate a sequence of tokens using a faster draft method, e.g., generation with a smaller model, as detailed in §4.1. The drafted tokens are then verified by the original model before being accepted as tokens of the original model. Since the verification can be performed on multiple tokens in parallel, its time is similar to or less than that of generating a single token if GPU computation is not the bottleneck. Thus, if tokens are accepted, speculative decoding is much faster than the original generation, as shown in the right half of Figure 5 (b). On the other hand, if the verification shows a different token than the drafted one, e.g., the 5th token for request 3 in our example, the drafted tokens 5–6 will be discarded and the drafter starts from token 6—as the verification will output the correct 5th token.

Challenge #1: Limited speedup for typical training configurations. While intuitive, adopting state-of-the-art speculative decoding techniques [2, 12, 26, 37] in rollout results in limited speedup, especially during the initial phase of rollout, because it is unfriendly to relatively large batch sizes common in training. Figure 6 (a) shows the distribution of per-worker batch sizes collected from production post-training jobs, and (b) shows the speedup of speculative decoding (Spec. D): we can see that for common batch sizes (e.g., 256), speculative decoding brings no or negative speedup. The reason is that the verification time increases more significantly with the batch size than others, as shown in Figure 5 (d), bottlenecked by the computational capabilities. Thus the verification costs offset the benefits (see Figure 5 (a)).

One may notice that the per-worker batch size decreases during rollout as more requests are finished, as shown in Figure 5 (a). However, we found that about 20% of the requests execute under relatively large batch sizes in our DAPO-32B-20K trace (see §5.1), which is unfriendly to speculative decoding that requires acceleration.

Our solution: dynamic decoupled speculative decoding (§4.1).

Our observation is that existing speculative decoding fails to fully utilize GPUs for computation-intensive verification, because much time is spent executing drafting that underutilizes GPUs, as shown in Figure 5 (c). An intuitive solution is to disaggregate the draft and verification jobs such that we can configure the GPU time in a more flexible way, as shown in Figure 5 (c). However, the current strict draft–verification dependency obstacles verification from utilizing the allocated GPU time: the verification must wait for drafting a sequence of tokens to reduce waste due to mis-speculation. To this end, our decoupled execution further relax such a dependency: as

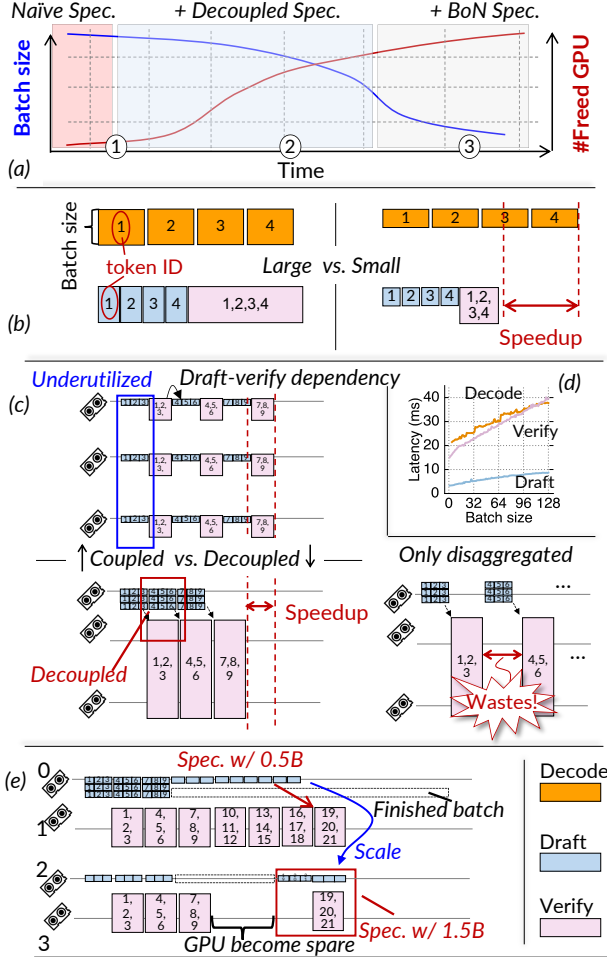


Figure 5: (a) An illustration of the rollout execution pattern and our acceleration method. (b) An illustration of why speculative decoding has limited speedup for large batches. (c) An illustration of the speedup brought by decoupled speculative decoding. (d) An analysis of the execution efficiency with respect to different batch sizes. (e) An illustration of the Best-of-N speculation method.

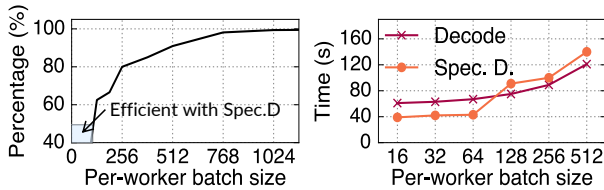


Figure 6: (a) Distribution of the initial per-worker batch sizes of post-training traces in the last 6 months in a large production cluster. (b) The acceleration of speculative decoding given such a batch size.

shown in (c), we continuously execute drafting and verification in a pipelined manner regardless of the drafting progress, which fully utilizes all GPU time for verification and enables efficient execution even with large batch sizes.

Decoupled speculative decoding faces the challenge of wasting more GPU resources upon mis-speculation. In the example in Figure 5 (c), if a token in positions 1–3 is mis-

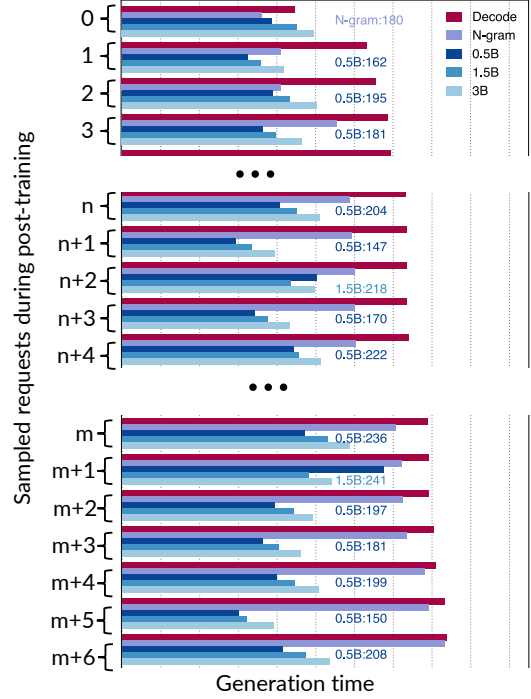


Figure 7: A characterization of the speedup of different drafting methods on DAPO-32B-20K (see §5.1) training trace.

speculated, extra drafted tokens (4–6) will be discarded. Fortunately, we found it has little impact on many requests since their acceptance rates remain high, so the speedup of decoupled execution offsets the loss due to waste, still enabling a rapid reduction in the per-worker batch size. To further cope with requests that suffer from significantly decreased acceptance rates, we only relax the draft-verification dependency without breaking it, and we dynamically control the degree of relaxation to balance the cost and fall back to coupled execution if necessary. The switched coupled execution is efficient thanks to the quickly reduced batch size due to decoupled execution.

Challenge #2: Selecting the best drafting methods without priori knowledge (§4.2). As mentioned in the introduction, selecting the best drafting method is critical to ensure high speedup yet is quite challenging because the optimal drafting method for each prompt varies and is unknown a priori. The diversity stems from the variation in acceptance rates for a given request. Figure 7 illustrates the speedup of different drafting methods on different requests from a batch collected from the training trace. We can see that although many requests achieve the highest speedup with 0.5 B drafting models, some require 1.5 B models and others require statistical methods like n-gram. Naively executing multiple drafting methods in parallel is infeasible because it requires significantly more GPUs—not only do we need to deploy multiple drafting models, but also the more costly verification process to verify the outputs from multiple drafting methods. *Our solution: dynamic Best-of-N speculation.* At the initial

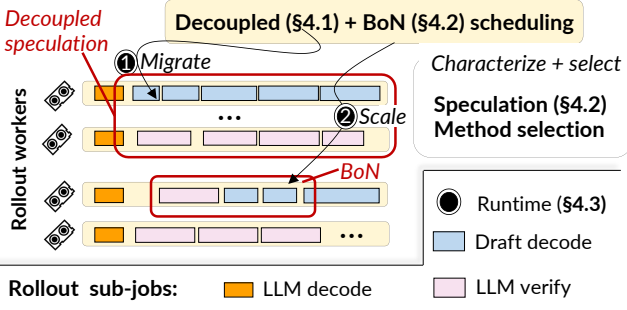


Figure 8: The system architecture of SPECACTOR.

phase of the rollout, we use the profiled acceptance rate to select the estimated best drafting method, based on the observation that although each prompt’s acceptance rate varies significantly, the average acceptance rate is statistically stable for a large batch. Therefore, the selection based on the average acceptance rate is likely to be close to the optimal for the batch. The best draft is selected based on a ladder we constructed offline, which holistically considers major methods, including model-based [25] and statistics-based [2, 12], detailed in §4.2.

During the rollout, when more GPUs are freed due to finished requests, SPECACTOR dynamically utilizes freed GPUs to deploy more drafting methods for tailed requests, where parallel drafting naturally approximates the best drafting method better. As shown in Figure 5 (e), if GPU 2 becomes spare, we add the second-best drafting method (1.5 B) to accelerate the unfinished requests on GPU 0.

System architecture. Figure 8 shows the system architecture of SPECACTOR: A global scheduler determines an efficient decoupled speculation plan (§4.1) during the initial rollout phase, and it dynamically reconfigure the execution pattern for low-acceptance-rate requests to improve efficiency. It further dynamically monitors the GPU usage of all workers and adds more drafting methods for long-tailed requests (§4.2). Finally, our runtime (§4.3) efficiently supports the *migrate* and *scale* primitives required for enforcing the above scheduling decisions.

4 Detailed Design and Implementation

4.1 Decoupled speculative decoding for rollout

Design rationale. We adopt a two-step scheduling method to realize an efficient decoupled speculation: (1) at the beginning of the rollout step, we determine the placement configurations—how many workers are assigned to drafting and verification—to maximize execution efficiency. During rollout, we (2) dynamically monitor the acceptance rate of different requests to timely adjust their execution patterns (e.g., variants of decoupled vs. coupled execution) to minimize the impact of verification failures. A batch-based formulation ensures high computation efficiency at the initial phase of rollout, while a per-request adaptation naturally optimizes tail

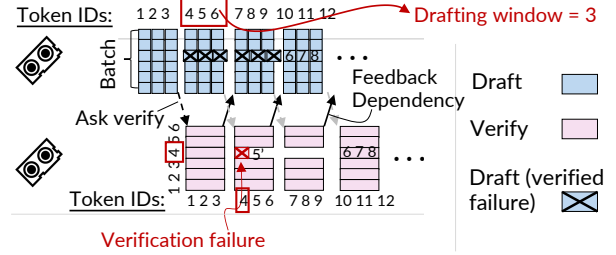


Figure 9: An illustration of the relaxed decoupled execution with a drafting window of 3 tokens.

requests, where optimization for computation efficiency is not the first priority.

We choose to dynamically configure the drafting window but not the entire placement during rollout for three reasons. First, the modeling of system execution becomes less accurate due to the continuously reduced batch sizes caused by finished requests, and second, the overhead of reconfiguring placement may outweigh the benefits, especially when the system has free GPUs. Finally, since the batch sizes shrink quickly with our initial placement, we no longer need to maximize the computational efficiency and fine-grained adjustment of the tail requests provided by (2) enables sufficient speedups.

Below, we first describe how we control the wasted tokens via relaxed decoupled execution and *draft window*, then we proceed to the two aforementioned policies.

Drafting window (w) and relaxed draft–verification dependency. To control the waste due to mis-speculation, we set a window such that: once the drafter drafts w tokens, it must send them to the verifier for verification. More importantly, the drafter is only allowed to continuously draft w tokens and wait for the feedback from the verifier. In this way, during speculation failure, the drafter only wastes a maximum of $2 \times w - 1$ tokens, as shown in Figure 9.

Setting the drafting window is tricky: it cannot be too small—because otherwise speculative decoding loses its advantage. Meanwhile, it cannot be too large—because it leads to wasted GPU computational intensity upon mis-speculation. Our policies about how to set the w properly is described below.

Decoupled speculation execution plan. At the beginning of each rollout step, given a draft method, the trained model, and the available GPUs, the planner decides an appropriate drafting window for the entire batch, and an efficient initial decoupled speculation plan by assigning drafter and verifier to different GPUs. The plan only needs to be executed once during post-training because for each step, the initial batch size per worker is the same and the prompts have similar lengths. Meanwhile, we found that the average acceptance rate—that impacts the drafting window selection—changes little between steps.

Finding the optimal execution plan requires solving a combination problem of the parallel configurations of different

Algorithm 1: Decoupled execution plan generation algorithm. $\text{TGS}_{g_d, g_v, w}(b)$, $V_{g_v, w}(b)$ and $D_{g_d}(b)$ are described in §4.1.

Input: Initial global batch size B , the number of GPUs in the cluster G , a set of execution configurations for verification \mathbb{G} .

Output: GPUs for drafting g_d^* , GPUs for verification g_v^* and draft window w^* .

- 1 $\text{TGS}^* \leftarrow 0, (g_d^*, g_v^*, w^*) \leftarrow (0, 0, 0)$
- 2 **foreach** GPU number $g_v \in \mathbb{G}$ **do**
- 3 **foreach** GPU number $g_d \leftarrow 1$ **to** g_v **do**
- 4 $b \leftarrow \lceil \frac{(g_d+g_v)B}{G} \rceil$
- 5 $w_{\max} = \max\{\lceil \frac{V'_{g_v, w}}{D'_{g_d}} \rceil, \lceil \frac{\beta_{g_v, w}}{\alpha_{g_d}} \rceil\}$
- 6 **for** $w \leftarrow 1$ **to** w_{\max} **do**
- 7 $\text{TGS}_{\text{cur}} \leftarrow \text{TGS}_{g_d, g_v, w}(b)$
- 8 **if** $\text{TGS}_{\text{cur}} > \text{TGS}^*$ **then**
- 9 $\text{TGS}^* \leftarrow \text{TGS}_{\text{cur}}$
- 10 $(g_d^*, g_v^*, w^*) \leftarrow (g_d, g_v, w)$

11 **return** (g_d^*, g_v^*, w^*)

drafters and verifiers, as well as precisely modeling the performance of speculative decoding using the drafting window. To ease problem formulation, we follow prior works that assume the developers have provided a set of possible GPU configurations for verification (\mathbb{G}), i.e., how one copy of model parameter is partitioned on a set of GPUs. For drafter, we assume it only uses one GPU as it is small.

Algorithm 1 describes our plan generation algorithm, which is essentially an enumeration-based search with decoupled-execution-aware pruning to accelerate the process. First, given a batch of requests to generate (i.e., B), we select a verification configuration (line 2), and estimate its performance under decoupled execution (TGS_{cur}) for various numbers of draft GPUs (line 3) and various drafting window sizes (line 6). We continuously select execution plans and finally choose the one with the minimal estimated generation time (line 8–10).

To improve search time, we prune the enumeration space by (1) using the observation that drafters need fewer GPUs than verifiers (line 3) and (2) we cannot choose an arbitrarily large drafting window, because it not only increases the computation waste upon mis-speculation (line 5).

Modeling TGS. A key aspect of our algorithm is to model the performance—token generation speed (TGS)—for decoupled execution. We use a bottom-up approach that first models the execution time of drafter and verifier then move on the modeling of the expectation of TGS, considering the impact of wasted tokens due to mis-speculation.

Given a batch of request b , the number of drafter workers g_d , and a verifier with execution configuration g_v , the draft

and verification time can be approximated as an affine function with respective to the batch size:

$$D_{g_d}(b) = b \cdot D'_{g_d} + \alpha_{g_d}$$

$$V_{g_v, w}(b) = b \cdot V'_{g_v, w} + \beta_{g_v, w}$$

where D'_{g_d} , $V'_{g_v, w}$, α_{g_d} and $\beta_{g_v, w}$ are hyperparameters that fitted through offline profiling, similar to prior works [72].

Therefore, the total generation time of w tokens in our decoupled execution paradigm can be modeled as:

$$\text{IL}_{g_d, g_v, w}(b) = \max\{wD_{g_d}(b), V_{g_v, w}(b)\}$$

Besides the generation time, the speed also needs to consider the number of tokens generated, including the wasted tokens due to mis-speculation. Given a drafting window w and the probability of accepting one token p for a batch of requests, we follow prior works [18, 32] that first model the probability of accepting a tokens given n tokens within a drafting window, then calculate wasted tokens accordingly. The difference is that we further consider the additional wasted tokens due to decoupled execution. Specifically, within a drafting window, the probability of accepting a tokens given an estimated accept probability (p) is:

$$P(a, w) = \begin{cases} p^a(1-p), & 0 \leq a \leq w-1, \\ p^a, & a = w, \end{cases}$$

s.t. $a \in \mathbb{N}, n \in \mathbb{Z}^+$

p can be profiled offline and we found it is quite stable for a relatively large batch of requests.

The expectation of the total generated tokens for drafting a draft window w is:

$$\tau_w = \sum_{a=0}^{w-1} p^a(1-p) \overbrace{\frac{a+1}{2}}^{\text{partial accept}} + \overbrace{wp^w}^{\text{full accept}}$$

which is a summation of the expected generated tokens when the token is accepted at different positions.

Put it all together, the expectation of TGS is:

$$\text{TGS}_{g_d, g_v, w}(b) = \frac{\tau_w}{\text{IL}_{g_d, g_v, w}(b)}$$

Dynamic request-level reconfiguration. During decoupled execution, we dynamically monitor each request’s acceptance rate to adjust its draft window size and execution mode (coupled vs. decoupled) accordingly. Algorithm 2 summarizes our reconfiguration algorithm, which is called periodically during the rollout.

Upon invocation, the algorithm first examines the set of requests with lower acceptance rates than the average (line 1), and reuses the performance model described above for decoupled execution and an extended modeling of coupled execution ($\text{TGS}_{C, w}()$, omitted due to space limitation, since

Algorithm 2: Request-level Reconfiguration for Reducing mis-speculation overheads

Input: pre-searched decoupled plan (g_d^*, g_v^*, w^*) , the set of requests with lower acceptance rate than average \mathbb{R} .

Output: Per-request draft plan $\{(w_r, m_r)\}_{r \in \mathbb{R}}$, w_r is request draft window, m_r is a flag specifying coupled (C) or decoupled (D) speculation.

```

1 foreach request  $r \in \mathbb{R}$  do
2    $p \leftarrow \text{ProfileProbability}(r)$ 
3    $w_c, \text{tgs}_c \leftarrow \arg \max_w \text{TGS}_{c,w}(p, b = 1)$ 
4    $w_d, \text{tgs}_d \leftarrow \arg \max_w \text{TGS}_{g_d^*, g_v^*, w}(p, b = 1)$ 
5    $w_r, m_r \leftarrow \text{SelectBetter}((w_c, \text{tgs}_c), (w_d, \text{tgs}_d))$ 
6 return  $\{(w_r, m_r) : r \in \mathbb{R}\}$ 

```

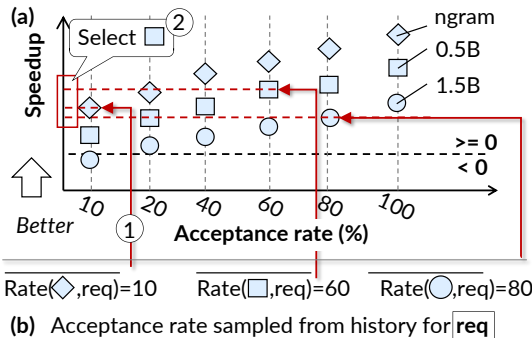


Figure 10: (a) A draft ladder providing hints to the speedup of different methods and (b) our rank (①) and then select (②) method to choose a drafting method.

its modeling logic is similar to decoupled modeling) to enumerate the best configuration.

Three things need to be noted about online reconfiguration. First, we do not trigger reconfiguration too frequently because (1) the acceptance rate may change sharply over a short term and (2) a too-frequent reconfiguration may introduce unstable performance. Currently, we configure the requests per 1000 generations. Second, even a request’s draft window is adjusted, it is still execute with requests with different draft window in a batch to maximize the GPU efficiency. To realize efficient co-execution, we scheduled the kernels if different drafting window CUDA graph [1, 32]. Finally, switch to coupled from decoupled execution is simple as we only need to pause the switched request’s aggressive draft.

4.2 Best-of-N (BoN) speculative decoding for rollout

This section describes how we select drafting methods for the rollout given the uncertainty of the best draft method. The goal is to select the method with the largest speedup, where the challenge is how to balance the draft efficiency and acceptance rate, and the acceptance rate is unknown before

execution for a request.

To cope with the above challenge, we leverage the fact that it is possible to estimate the speedup of different draft methods via offline profiling. With this information, selecting drafting methods greedily using average acceptance rate of a batch request is possible since the average rate is relative stable.

Draft ladder. A draft ladder provides information on the speedup of different draft methods given a fixed acceptance rate, as shown in Figure 10 (a). It can be efficiently constructed via offline profiling without using the trained model because (1) the execution of the drafter is irrelevant to the training model and (2) the verification overhead can be simulated by randomly marking tokens as accepted or rejected according to the acceptance rate. Therefore, during offline profiling, we follow the above two steps to build the draft ladder. Specifically, our ladder considers popular drafting methods for speculative decoding, including model-based [25] and n-gram based [2, 12]. We are continuously adding more drafting models including training-based speculation methods such as the Eagle family [26, 27] and MTP [9], and these integration would likely to make SPECACTOR faster.

Initial selection. At the start of each rollout, we select one draft method for the entire batch based on the historically profiled acceptance rate. We cannot support multiple methods because each drafter requires the same amount of verification, and we have insufficient GPU computation power during the initial phase.

Figure 10 (b) presents our selection process. For three exemplified draft methods—ngram, drafting with a 0.5 B and 1.5 B model, we first query the historical acceptance rate of these methods, and use these rates as the estimated acceptance of the batch. For each model, we use its rate to query the speedup from the ladder (①) and select the largest one (②) as the initial drafting method.

Greedy Best-of-N assignments. To cope with the sub-optimal initial selection for tailed requests, we greedily deploy more drafters when some requests finish and GPUs are released. Algorithm 3 shows our simplified algorithm for assigning more drafters (and their corresponding verifier) when there are available workers. The routine is iteratively called once there is available workers freed. Our presented method assumes deploying a drafter and its verifier using a fashion; in practice we found decoupled execution is slightly faster though the detailed assignment method becomes somewhat complex. Since the rationale is similar, we only present assignments of coupled execution and briefly describe extension to decoupled assignment.

Upon receiving freed workers where each worker is capable of running a verifier using the configuration described in §4.1, our global scheduler tries its best to assign a drafter to each worker (lines 1–3). Afterward, it assigns drafters to requests in a greedy manner where the request with the

Algorithm 3: Greedy Best-of-N assignments. The maximum verification batch b_{max} is pre-defined.

Input: the active requests set \mathbb{R} , the candidate draft methods set \mathbb{D} , and freed rollout workers \mathbb{W} . \mathbb{W}_d is the existing worker set responsible for draft method d .

Output: added drafters and the involved requests $\mathcal{M} = \{(r, d) : w\}_{r \in \mathbb{R}, d \in \mathbb{D}, w \in \mathbb{W}}$.

```

1 foreach worker  $w \in \mathbb{W}$  do
2   draft method  $d \leftarrow \arg \min_d |\mathbb{W}_d|$ 
3    $\mathbb{W}_d \leftarrow \mathbb{W}_d \cup \{w\}$ 
4 foreach draft method  $d \in \mathbb{D}$  do
5    $\mathcal{R} \leftarrow$  sort  $\mathbb{R}$  by GetAcceptRate(r) ascending
6   foreach worker  $w \in \mathbb{W}_d$  do
7     while  $load(w) < b_{max}$  and  $|\mathcal{R}| > 0$  do
8        $r \leftarrow pop(\mathcal{R})$ 
9        $\mathcal{M}(r, d) \leftarrow w$ 
10       $load(w) += 1$ 
11 return  $\mathcal{M}$ 

```

lowest acceptance rate (lines 4–5) is processed first. After assigning one drafter (and a corresponding verifier) to a freed worker, the worker’s computation capacity is updated (lines 9–10). If a worker has insufficient capacity as measured by the current verification batch size, the request is skipped. To support decoupled assignment, we need to further consider the placement of drafter workers that may co-execute with existing drafters.

We adopted a depth-first-based solution that assigns all drafters to one request before moving on to the next. The rationale here is that the request with the lowest acceptance rate is likely to be the slowest one, so DFS can approximate quickly assign the best drafting method for acceleration. Moreover, when more requests finish, the remaining requests can utilize their GPUs so other tail requests would be considered.

4.3 Efficient runtime mechanisms for SPECACTOR

SPECACTOR runtime provides two basic primitives to support dynamic job reconfigurations, whose detailed mechanisms are similar to their counterparts in inference systems with a few our customizations for the rollout.

Model scale. Scale deploys a serving instance of a specific model—e.g., a draft model in SPECACTOR—to a rollout worker, e.g., to add a drafter for a request. The detailed scaling process is similar to model autoscaling in inference systems [13, 58, 54, 64, 65] with control and data planes: the control plane initializes the framework runtime (e.g., Python) and prepares the CUDA graphs, while the data plane loads model parameters to the GPUs.

To accelerate drafter deployment, SPECACTOR adopts all

current optimizations for autoscaling, including pre-pinning the serving engine on each worker to avoid initializing the runtime from scratch [58], pre-materializing CUDA graphs with GPU execution context pools [64, 54]—which is always possible in rollout since the supported models are known in advance—and loading parameters from the compute fabric between workers with cached model parameters in the global GPU-CPU pool [65]. Additionally, unlike BlitzScale, which only caches one parameter copy of each model in the cluster, SPECACTOR caches all models on host DRAM of all workers to enable the dataplane to always use the fastest links (PCIe and NVLink broadcast). This is possible because SPECACTOR only needs to support a few draft models, and each worker’s host DRAM is sufficient to cache them, e.g., all draft models of a 32 B rollout have 4 GB parameters in total. Finally, we store the trained models GPUs of all workers (including drafters) to avoid the dataplane costs since the parameters of the trained model is relative large.

KVCache scale. Besides the model, when scaling a new drafter’s corresponding verifier, the new verifier needs a copy of the KVCache—the intermediate results of the LLM computation—to accelerate computation. A challenge is that during the later stage of rollout, the KVCache may become large since it is proportional to the model size. To this end, we leverage the classic KVCache recovery method that transfers the tail KVCache through the network and recomputes it from the beginning [21] to accelerate the KVCache scaling.

5 Evaluation

5.1 Experimental setup

We implemented SPECACTOR on veRL—the state-of-the-art training framework for post-training that has integrated known inference optimizations including including CUDA graph, prefix caching [45] and FlashAttention kernels [44] for fast rollouts.

Testbed. We evaluate SPECACTOR on a production training cluster with up to 512 GPUs. These GPUs are organized into nodes where each node contains eight Hopper (80 GB) GPUs interconnected with 400 GB/s NVLink, and inter-node GPUs have up to 400 Gbps RDMA connections.

Evaluated traces. Similar to prior works [61, 46, 69], we evaluate Qwen series models (e.g., Qwen2.5-32B) as they are popular high-accuracy open-sourced LLMs [61, 62, 68] and are selected by algorithm designers. We evaluate on two representative training traces based on real-world training setups:

- **GRPO-32B-20K.** This trace trains Qwen2.5-32B [53] with the GRPO [45] algorithm, a representative value-model-free post-training method that trains high-quality models like DeepSeek series [66, 8]. The trace samples a total batch of 8,192 prompts at each step², where for each

²Including the group sampling factor.

batch, the model generates responses with a maximum length of 20 K tokens. The trace runs on 256 GPUs with a tensor parallelism (TP) degree of 4 for each rollout worker, so the initial per-worker batch size is 128.

- **DAPO-32B-20K.** This trace also trains Qwen2.5-32B using DAPO [61]—a trending algorithm in AI academy and industry [15, 59]—with a per-step total batch size of 16,384 and a maximum response length of 20 K tokens. The trace still runs on 256 GPUs with a TP degree of 4 for each rollout worker, so the per-worker batch size is 256. DAPO requires a larger per-step batch size because its training method filters out low-quality responses generated during the rollout.

Evaluating metrics. We focus on reporting the end-to-end training time and the rollout time—since training time is the most critical metric for algorithm developers and rollout dominates the time in §2.1. Due to the availability of GPU clusters, we sample at least 10 % of the total training steps uniformly across all steps, using the trained checkpoints at the sampled steps for generation, and report their training and rollout time.

Baselines. We compared SPECACTOR with the following baselines and carefully tuned their implementations and performance. Specifically, the decoding latency of Qwen2.5-32 B model is lower than 13 ms when the batch size per worker is one for all baselines. Notice we set sampling temperature to 1 following common post-training practice. For all baselines, we configure the same optimal configuration for the preparation and learning phases, i.e., an FSDP degree of 32 and sequence parallelism [19] of degree eight.

- **veRL** [47] is an open-sourced post-training system used by SEED and SPECACTOR is based on it. Besides the inference optimizations mentioned in the beginning of the section, it further incorporates techniques like efficient parameter to quickly update parameters for the rollout.
- **RLHFuse** [70] is the state-of-the-art post-training system that overlaps the preparation and rollout phases to reduce bubbles caused by tailed generation in the rollout. Since it is not open-sourced, we carefully re-implemented its design in state-of-the-art and achieve a similar speedup on short-generation tasks.
- **veRL (2 ×)** provisions 2 × of GPUs used by the original trace for veRL, which serves as the optimal performance of using more GPUs to accelerate rollout like RLBoost [6].
- **veRL + VanillaSpec** [25]. To illustrate the effectiveness of our proposed techniques, we also compare veRL by incorporating model-based speculation decoding acceleration in inference systems. The implementation is based on the latest vLLM [1], and we ports coupled speculation described in §3. The drafting method is selected based on the first

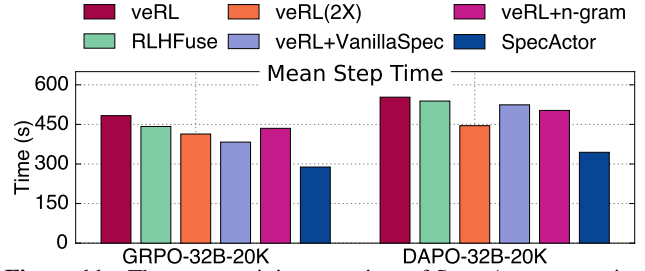


Figure 11: The mean training step time of SPECACTOR running different training traces with different approaches.

phase of our Best-of-N speculation. For example, for 32B training, we found 0.5B is a sweet point to accelerate.

- **veRL + n-gram.** N-gram is a category of training-free draft methods. It adopts dynamic token cache to retrieve redundant sequences from recent outputs [57, 50]. We integrate vLLM’s n-gram implementation into veRL as a speculative decoding baseline to illustrate how n-gram-based methods [2, 12, 34] work in accelerating rollout, similar to a recent work [16].

Draft methods used by SPECACTOR. We choose the three methods for the drafter of Qwen 2.5-32B training as: Qwen2.5-0.5B [53], Qwen2.5-1.5B, n-gram [1]. Other draft models are too slow so we neglect them.

5.2 End-to-end post-training performance

Figure 11 presents the end-to-end training step time of different approaches on the traces. We measure all sampled training steps and report the mean step time of different approaches. SPECACTOR achieves 1.3 × shorter end-to-end training time compared to the best baseline (i.e., veRL + VanillaSpec for GRPO and veRL (2 ×) for DAPO), and achieves 1.5–1.7 × shorter time compared to others. The key contributor is the acceleration of rollout time via our efficient speculative rollout: for the rollout phase, SPECACTOR achieves 2.0–2.4 ×, 1.8–2.3 × faster generation speed than veRL, veRL (2 ×); note that veRL (2 ×) uses twice the GPUs of SPECACTOR.

Notably, SPECACTOR achieves 1.7–2.0 × shorter rollout time even compared with methods that also incorporate speculative decoding acceleration, i.e., VanillaSpec and n-gram. This is because: First, both of them suffer from inefficiency due to large per-worker batch size during the initial rollout phase. Second, both of them, especially n-gram, have low acceptance rates for the straggler requests, because the n-gram method performs poorly in high temperature sampling with few history prompts commonly found in training traces. Specifically, the acceptance rate of the last finished requests of n-gram is almost zero on both traces, while SPECACTOR achieves 48.7–72.3 % acceptance rate.

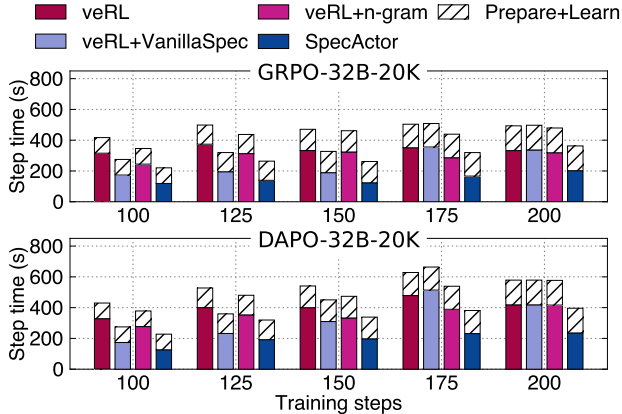


Figure 12: A breakdown of post-training process of different approaches on different training traces.

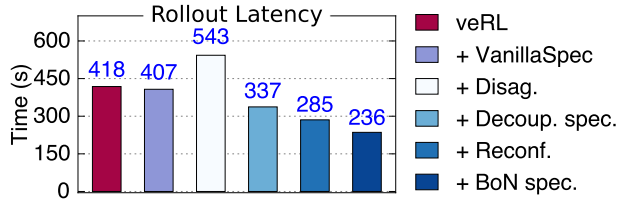


Figure 13: Ablation study of using the DAPO-32B-20K trace. The other trace shows similar results.

5.3 Performance across different steps

As the trained model evolves across different training steps, the effectiveness of speculative decoding varies. Thus, we further present the detailed latency breakdown of different training steps in Figure 12. For ease of presentation, we selectively present part of the training steps between 100–200 training steps to examine speculative decoding’s effect in real-world post-training. The gap is sufficiently large as confirmed by internal accuracy tests, so the “smartness” of the trained models in different sampling steps varies.

First we can see that SPECACTOR still achieves the fastest rollout time in all steps. Specifically, at 175th and 200th steps, veRL + VanillaSpec and n-gram fail to provide acceleration because as the model becoming smarter, they tend to produce long generations [8] for more prompts, so most of the rollout time executes with a relative large per-worker batch size. In contrast, SPECACTOR consistently reduces rollout time by 1.7–2.4 \times . Thanks to the quick generation, more workers finish at early time, leaving SPECACTOR sufficient room for BoN scheduling.

5.4 Ablation study

Figure 13 conducts an ablation study to examine the effectiveness of different proposed techniques described in §4. We reported only one step here due to space limitation, and other steps show similar results.

First, we can see that vanilla speculative decoding reduces only 2.6 % rollout end-to-end latency, which is small due to the inefficiency of large-batch verification and suboptimal

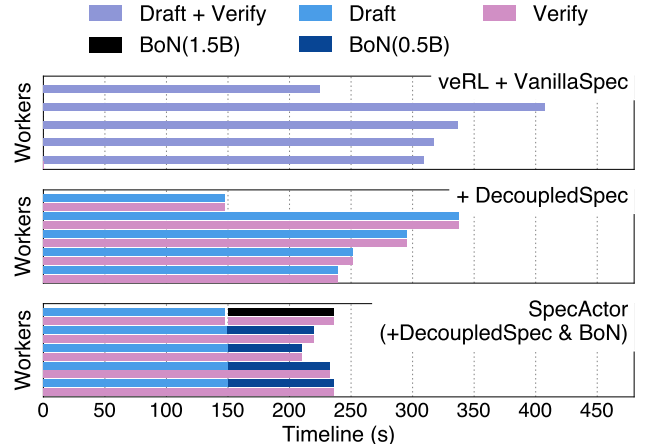


Figure 14: An in-depth analysis of the execution of different approaches on the 200th step of DAPO-32B-20K training trace. We sample workers that contains the tailed requests for ease of presentation.

drafting method for the tailed requests. Naively disaggregating draft and verification jobs described in §3 to improve the execution efficiency provides negative speedup (33.4 % longer rollout time) because disaggregating but not decoupling adds substantial GPU wait time (see Figure 5 (c)).

Thanks to our decoupled speculative decoding, we accelerate rollout by 1.3 \times . Based on decoupled speculative decoding, our dynamic reconfiguration further shortens the rollout time by 1.2 \times thanks to a better initial execution configuration and dynamic reconfiguration of workers with low acceptance rates to reduce wasted tokens. Finally, our Best-of-N speculative decoding further accelerates end-to-end rollout by 1.2 \times , thanks to its ability to leverage multiple draft methods to improve acceptance rates for straggler requests.

5.5 An In-depth Look at SPECACTOR in action

We conclude our evaluation of SPECACTOR by presenting an in-depth analysis of the work done by different workers during the rollout with our techniques in Figure 14. To ease presentation, we only sampled 5 workers, with a deliberate focus on the worker that finish early and the slowest four workers.

First, from the first row of Figure 14 we can see that vanilla speculative decoding still suffers from long-tailed workers because during the initial phase all workers execute slower and at the end the initially selected drafting method cannot accelerate the slowest requests. With decoupled speculative decoding (the second row), we improve speculative decoding performance by 1.1–1.5 \times but still suffer from long-tailed requests due to suboptimal drafting method. With Best-of-N speculative decoding activated, the freed workers are assigned different drafting methods (we use different color blocks to indicate different drafting methods) at the 151st second. This subsequently accelerates the slowest requests by 1.5 \times .

Table 1: A comparison of various post-training acceleration methods described in §7.

Systems	Algorithm-agnostic	No extra GPU	Rollout performance
veRL [46]	✓	✓	Low
RLHFuse [70]	✓	✓	Low
RLBoost [6]	✓	✗	Medium
StreamRL [69]	✗	✓	Low
AReAL [11]	✗	✓	Low
RhymeRL [16]	✗	✓	Medium
RollPacker [14]	✗	✓	Low
This work	✓	✓	High

6 Discussion

Supporting larger models. Due to the limited GPU budget, we only present results on dense models such as Qwen2.5. Nevertheless, our methodology also applies to larger MoE models like Qwen3-235 B, which is confirmed by our initial evaluations. We will release related results in the next version of our paper.

Supporting evolvable draft methods. During the training process, the trained model becomes smarter and one may wonder whether this could lead to decreased speculation acceptance accuracy. Surprisingly, we found that the acceptance rate remains stable not only between adjacent steps but also steps apart (e.g., 100) for different methods. We suspect this is because even though the capability gap between the trained model and the drafter becomes larger during the training process, there are still many trivial tokens that can be drafted. Meanwhile, we could also evolve the drafter by training it together with the target model since the evolving method is similar to the prepare + learn phases described in §2. The additional overhead is negligible because (1) the original prepare+learn time is much smaller than the rollout and (2) the drafter requires orders of magnitude less computational power for these phases when compared with the trained model [30]. We plan to explore evolvable drafters in the future.

7 Related work

Post-training acceleration without algorithmic changes. As we have extensively discussed in §2.2, current works that accelerate post-training in an algorithmic way, either by overlapping [70, 6] or requiring more GPUs [6], offer limited speedup especially for long-tailed generations. SPECACTOR directly accelerates generations with rollout-tailed dynamic and decoupled Best-of-N speculation.

Post-training acceleration with algorithmic modifications. Several works propose algorithmic changes to accelerate rollout. Such modifications can slow convergence in theory [3, 41, 51] and SPECACTOR is orthogonal to these methods: they do not change the LLM generation process, whereas we directly

accelerate it without requiring additional GPUs.

Partial-rollout approaches [52, 4] set a token threshold and pause long-tailed generations in a step once the threshold is met. These generations are resumed in future training steps, which essentially turns training from on-policy to off-policy, similar to AReAL [11], that suffers from loss of accuracy as discussed in §2.1. RollPacker [14] further packs long-tailed generations that were previously truncated together to reduce bubble time, which changes the batch formulation so it may change the training dynamics [56, 48]. Besides, it cannot eliminate the long-tailed generations since these generations also differ in length.

Inference acceleration with speculative decoding. Speculative decoding is a widely-adopted technique to accelerate token generation in LLM serving [26, 27, 23, 37, 29, 67, 30]. To the best of our knowledge, existing approaches do not target execution efficiency for large batches (e.g., SpecInfer [37] accelerates requests with batch sizes no larger than 16) or the diverse drafting methods required in post-training rollout, which we addressed. Moreover, inference can use approximate speculative sampling to further improve acceptance rate [57], while post-training requires exact matching to ensure training correctness [31]. This calls for more advanced speculation methods to improve accuracy, so we proposed Best-of-N speculation.

Our decoupled speculation—at a first glance—is conceptually similar to parallel drafting and verification in PEARL [29] and SwiftSpec [67], but with two significant distinctions: (1) we maximize the batch computational efficiency, while they only consider the algorithm-side design for a single request and (2) we provide a systematic approach to improve the speculation efficiency rate with dynamic adaption and Best-of-N speculation which is required for rollout due to the lower acceptance rate resulting from the rigorous verification requirement described above.

8 Conclusion

This paper shows that rollout in post-training can be efficient without compromising the training quality of large language models with efficient speculative rollout. SPECACTOR makes speculative decoding efficient for rollout with two techniques: a dynamic decoupled speculation method that improves the efficiency of speculative decoding for large batch sizes, with refinements for handling the decreased acceptance rate for tail requests, and (2) a Best-of-N speculation method that enhances the acceptance rate of speculation. SPECACTOR improves the training efficiency by 1.3–1.7 × compared to the state-of-the-art baselines, and is 1.5 × faster than naively utilizing speculative decoding for rollout.

References

[1] Easy, fast, and cheap llm serving for everyone. <https://github.com/vllm-project/vllm>, 2024.

[2] APOORV SAXENA, A. T. S. Prompt lookup decoding. <https://github.com/apoorvumang/prompt-lookup-decodin>, 2025.

[3] ARNAL, C., NAROZNIAK, G., CABANNES, V., TANG, Y., KEMPE, J., AND MUNOS, R. Asymmetric REINFORCE for off-policy reinforcement learning: Balancing positive and negative rewards. *CoRR abs/2506.20520* (2025).

[4] BAI, Y., BAO, Y., CHEN, G., AND ET. AL. Kimi K2: open agentic intelligence. *CoRR abs/2507.20534* (2025).

[5] BAI, Y., JONES, A., NDOUSSE, K., AND ET.AL. Training a helpful and harmless assistant with reinforcement learning from human feedback. *CoRR abs/2204.05862* (2022).

[6] BATANERO, E. A., PASCUAL, Á. F., AND JIMÉNEZ, Á. B. Rl-boost: Boosting supervised models using deep reinforcement learning. *Neurocomputing 618* (2025), 128815.

[7] CHEN, C., BORGEAUD, S., IRVING, G., LESPIAU, J., SIFRE, L., AND JUMPER, J. Accelerating large language model decoding with speculative sampling. *CoRR abs/2302.01318* (2023).

[8] DAYA GUO, DEJIAN YANG, H. Z. E. A. Deepseek-r1 incentivizes reasoning in llms through reinforcement learning. *Nature 645* (2025), 633–638.

[9] DEEPSEEK-AI. Deepseek-v3 technical report. *CoRR abs/2412.19437* (2024).

[10] DEEPSEEK-AI, GUO, D., YANG, D., ZHANG, H., AND ET. AL. Deepseek-r1: Incentivizing reasoning capability in llms via reinforcement learning. *CoRR abs/2501.12948* (2025).

[11] FU, W., GAO, J., SHEN, X., ZHU, C., MEI, Z., HE, C., XU, S., WEI, G., MEI, J., WANG, J., YANG, T., YUAN, B., AND WU, Y. Areal: A large-scale asynchronous reinforcement learning system for language reasoning. *CoRR abs/2505.24298* (2025).

[12] FU, Y., BAILIS, P., STOICA, I., AND ZHANG, H. Break the sequential dependency of LLM inference using lookahead decoding. In *Forty-first International Conference on Machine Learning, ICML 2024, Vienna, Austria, July 21-27, 2024* (2024), OpenReview.net.

[13] FU, Y., XUE, L., HUANG, Y., BRABETE, A., USTIUGOV, D., PATEL, Y., AND MAI, L. Serverlessllm: Low-latency serverless inference for large language models. In *18th USENIX Symposium on Operating Systems Design and Implementation, OSDI 2024, Santa Clara, CA, USA, July 10-12, 2024* (2024), A. Gavrilovska and D. B. Terry, Eds., USENIX Association, pp. 135–153.

[14] GAO, W., ZHAO, Y., AN, D., WU, T., CAO, L., XIONG, S., HUANG, J., WANG, W., YANG, S., SU, W., WANG, J., QU, L., ZHENG, B., AND WANG, W. Rollpacker: Mitigating long-tail rollouts for fast, synchronous RL post-training. *CoRR abs/2509.21009* (2025).

[15] GOLUBEV, A., TROFIMOVA, M., POLEZHAEV, S., BADERTDINOV, I., NEKRASHEVICH, M., SHEVTSOV, A., KARASIK, S., ABRAMOV, S., ANDRIUSHCHENKO, A., FISIN, F., SKVORTSOV, S., AND YANGEL, B. Training long-context, multi-turn software engineering agents with reinforcement learning. *CoRR abs/2508.03501* (2025).

[16] HE, J., LI, T., FENG, E., DU, D., LIU, Q., LIU, T., XIA, Y., AND CHEN, H. History rhymes: Accelerating LLM reinforcement learning with rhymerl. *CoRR abs/2508.18588* (2025).

[17] HOEFFDING, W. Probability inequalities for sums of bounded random variables. *Journal of the American statistical association 58*, 301 (1963), 13–30.

[18] HUANG, Z., ZHU, L., ZHAN, Z., HU, T., MAO, W., YU, X., LIU, Y., AND ZHANG, T. Moesd: Unveil speculative decoding’s potential for accelerating sparse moe. *CoRR abs/2505.19645* (2025).

[19] JACOBS, S. A., TANAKA, M., ZHANG, C., ZHANG, M., SONG, S. L., RAJBHANDARI, S., AND HE, Y. Deepspeed ulysses: System optimizations for enabling training of extreme long sequence transformer models. *CoRR abs/2309.14509* (2023).

[20] JIMENEZ, C. E., YANG, J., WETTIG, A., YAO, S., PEI, K., PRESS, O., AND NARASIMHAN, K. R. Swe-bench: Can language models resolve real-world github issues? In *The Twelfth International Conference on Learning Representations, ICLR 2024, Vienna, Austria, May 7-11, 2024* (2024), OpenReview.net.

[21] JIN, S., LIU, X., ZHANG, Q., AND MAO, Z. M. Compute or load KV cache? why not both? *CoRR abs/2410.03065* (2024).

[22] KESKAR, N. S., MUDIGERE, D., NOCEDAL, J., SMELYANSKIY, M., AND TANG, P. T. P. On large-batch training for deep learning: Generalization gap and sharp minima. In *5th International Conference on Learning Representations, ICLR 2017, Toulon, France, April 24-26, 2017, Conference Track Proceedings* (2017), OpenReview.net.

[23] KWON, W., LI, Z., ZHUANG, S., SHENG, Y., ZHENG, L., YU, C. H., GONZALEZ, J., ZHANG, H., AND STOICA, I. Efficient memory management for large language model serving with pagedattention. In *Proceedings of the 29th Symposium on Operating Systems Principles, SOSP 2023, Koblenz, Germany, October 23-26, 2023* (2023), J. Flinn, M. I. Seltzer, P. Druschel, A. Kaufmann, and J. Mace, Eds., ACM, pp. 611–626.

[24] LEVIATHAN, Y., KALMAN, M., AND MATIAS, Y. Fast inference from transformers via speculative decoding. In *International Conference on Machine Learning, ICML 2023, 23-29 July 2023, Honolulu, Hawaii, USA* (2023), A. Krause, E. Brunskill, K. Cho, B. Engelhardt, S. Sabato, and J. Scarlett, Eds., vol. 202 of *Proceedings of Machine Learning Research*, PMLR, pp. 19274–19286.

[25] LEVIATHAN, Y., KALMAN, M., AND MATIAS, Y. Fast inference from transformers via speculative decoding. In *International Conference on Machine Learning, ICML 2023, 23-29 July 2023, Honolulu, Hawaii, USA* (2023), A. Krause, E. Brunskill, K. Cho, B. Engelhardt, S. Sabato, and J. Scarlett, Eds., vol. 202 of *Proceedings of Machine Learning Research*, PMLR, pp. 19274–19286.

[26] LI, Y., WEI, F., ZHANG, C., AND ZHANG, H. EAGLE-2: faster inference of language models with dynamic draft trees. In *Proceedings of the 2024 Conference on Empirical Methods in Natural Language Processing, EMNLP 2024, Miami, FL, USA, November 12-16, 2024* (2024), Y. Al-Onaizan, M. Bansal, and Y. Chen, Eds., Association for Computational Linguistics, pp. 7421–7432.

[27] LI, Y., WEI, F., ZHANG, C., AND ZHANG, H. EAGLE-3: scaling up inference acceleration of large language models via training-time test. *CoRR abs/2503.01840* (2025).

[28] LIU, B., WANG, A., MIN, Z., YAO, L., ZHANG, H., LIU, Y., ZENG, A., AND SU, J. Spec-rl: Accelerating on-policy reinforcement learning via speculative rollouts, 2025.

[29] LIU, T., LI, Y., LV, Q., LIU, K., ZHU, J., HU, W., AND SUN, X. PEARL: parallel speculative decoding with adaptive draft length. In *The Thirteenth International Conference on Learning Representations, ICLR 2025, Singapore, April 24-28, 2025* (2025), OpenReview.net.

[30] LIU, X., HU, L., BAILIS, P., CHEUNG, A., DENG, Z., STOICA, I., AND ZHANG, H. Online speculative decoding. In *Forty-first International Conference on Machine Learning, ICML 2024, Vienna, Austria, July 21-27, 2024* (2024), OpenReview.net.

[31] LIU, X., HU, L., BAILIS, P., CHEUNG, A., DENG, Z., STOICA, I., AND ZHANG, H. Online speculative decoding, 2024.

[32] LIU, X., PARK, J., HU, L., KWON, W., LI, Z., ZHANG, C., DU, K., MO, X., YOU, K., CHEUNG, A., DENG, Z., STOICA, I., AND ZHANG, H. Turbospec: Closed-loop speculation control system for optimizing llm serving goodput. *CoRR* (2025).

[33] LIU, X., YU, H., ZHANG, H., AND ET. AL. Agentbench: Evaluating llms as agents. In *The Twelfth International Conference on Learning Representations, ICLR 2024, Vienna, Austria, May 7-11, 2024* (2024), OpenReview.net.

[34] LUO, X., WANG, Y., ZHU, Q., ZHANG, Z., ZHANG, X., YANG, Q., AND XU, D. Turning trash into treasure: Accelerating inference of large language models with token recycling. In *Proceedings of the 63rd Annual Meeting of the Association for Computational Linguistics (Volume 1: Long Papers), ACL 2025, Vienna, Austria, July 27 - August 1, 2025* (2025), W. Che, J. Nabende, E. Shutova, and M. T. Pilehvar, Eds., Association for Computational Linguistics, pp. 6816–6831.

[35] MEI, Z., FU, W., LI, K., WANG, G., ZHANG, H., AND WU, Y. Realhf: Optimized RLHF training for large language models through parameter reallocation. *CoRR abs/2406.14088* (2024).

[36] MIAO, X., OLIARO, G., ZHANG, Z., CHENG, X., WANG, Z., ZHANG, Z., WONG, R. Y. Y., ZHU, A., YANG, L., SHI, X., SHI, C., CHEN, Z., ARFEEN, D., ABHYANKAR, R., AND JIA, Z. Specinfer: Accelerating large language model serving with tree-based speculative inference and verification. In *Proceedings of the 29th ACM International Conference on Architectural Support for Programming Languages and Operating Systems, Volume 3, ASPLOS 2024, La Jolla, CA, USA, 27 April 2024- 1 May 2024* (2024), R. Gupta, N. B. Abu-Ghazaleh, M. Musuvathi, and D. Tsafirir, Eds., ACM, pp. 932–949.

[37] MIAO, X., OLIARO, G., ZHANG, Z., CHENG, X., WANG, Z., ZHANG, Z., WONG, R. Y. Y., ZHU, A., YANG, L., SHI, X., SHI, C., CHEN, Z., ARFEEN, D., ABHYANKAR, R., AND JIA, Z. Specinfer: Accelerating large language model serving with tree-based speculative inference and verification. In *Proceedings of the 29th ACM International Conference on Architectural Support for Programming Languages and Operating Systems, Volume 3, ASPLOS 2024, La Jolla, CA, USA, 27 April 2024- 1 May 2024* (2024), R. Gupta, N. B. Abu-Ghazaleh, M. Musuvathi, and D. Tsafirir, Eds., ACM, pp. 932–949.

[38] NAKANO, R., HILTON, J., BALAJI, S., WU, J., OUYANG, L., KIM, C., HESSE, C., JAIN, S., KOSARAJU, V., SAUNDERS, W., JIANG, X., COBBE, K., ELOUNDOU, T., KRUEGER, G., BUTTON, K., KNIGHT, M., CHESS, B., AND SCHULMAN, J. Webgpt: Browser-assisted question-answering with human feedback. *CoRR abs/2112.09332* (2021).

[39] NOUKHOVITCH, M., HUANG, S., XHONNEUX, S., HOSSEINI, A., AGARWAL, R., AND COURVILLE, A. C. Asynchronous RLHF: faster and more efficient off-policy RL for language models. In *The Thirteenth International Conference on Learning Representations, ICLR 2025, Singapore, April 24-28, 2025* (2025), OpenReview.net.

[40] OPENAI. GPT-4 technical report. *CoRR abs/2303.08774* (2023).

[41] ROUX, N. L., BELLEMARE, M. G., LEBENSOLD, J., BERGERON, A., GREAVES, J., FRÉCHETTE, A., PELLETIER, C., THIBODEAU-LAUFER, E., TÓTH, S., AND WORK, S. Tapered off-policy REINFORCE: stable and efficient reinforcement learning for llms. *CoRR abs/2503.14286* (2025).

[42] ROZIÈRE, B., GEHRING, J., GLOECKLE, F., SOOTLA, S., GAT, I., TAN, X. E., ADI, Y., LIU, J., REMEZ, T., RAPIN, J., KOZHEVNIKOV, A., EVTIMOV, I., BITTON, J., BHATT, M., CANTON-FERRER, C., GRATTAIORI, A., XIONG, W., DÉFOSSEZ, A., COPET, J., AZHAR, F., TOUVRON, H., MARTIN, L., USUNIER, N., SCIALOM, T., AND SYNNAEVE, G. Code llama: Open foundation models for code. *CoRR abs/2308.12950* (2023).

[43] SCHULMAN, J., WOLSKI, F., DHARIWAL, P., RADFORD, A., AND KLIMOV, O. Proximal policy optimization algorithms. *CoRR abs/1707.06347* (2017).

[44] SHAH, J., BIKSHANDI, G., ZHANG, Y., THAKKAR, V., RAMANI, P., AND DAO, T. Flashattention-3: Fast and accurate attention with asynchrony and low-precision. In *Advances in Neural Information Processing Systems 38: Annual Conference on Neural Information Processing Systems 2024, NeurIPS 2024, Vancouver, BC, Canada, December 10 - 15, 2024* (2024), A. Globersons, L. Mackey, D. Belgrave, A. Fan, U. Paquet, J. M. Tomczak, and C. Zhang, Eds.

[45] SHAO, Z., WANG, P., ZHU, Q., XU, R., SONG, J., ZHANG, M., LI, Y. K., WU, Y., AND GUO, D. Deepseekmath: Pushing the limits of mathematical reasoning in open language models. *CoRR abs/2402.03300* (2024).

[46] SHENG, G., ZHANG, C., YE, Z., WU, X., ZHANG, W., ZHANG, R., PENG, Y., LIN, H., AND WU, C. Hybridflow: A flexible and efficient RLHF framework. In *Proceedings of the Twentieth European Conference on Computer Systems, EuroSys 2025, Rotterdam, The Netherlands, 30 March 2025 - 3 April 2025* (2025), ACM, pp. 1279–1297.

[47] SHENG, G., ZHANG, C., YE, Z., WU, X., ZHANG, W., ZHANG, R., PENG, Y., LIN, H., AND WU, C. Hybridflow: A flexible and efficient RLHF framework. In *Proceedings*

of the Twentieth European Conference on Computer Systems, EuroSys 2025, Rotterdam, The Netherlands, 30 March 2025 - 3 April 2025 (2025), ACM, pp. 1279–1297.

[48] SHUMAILOV, I., SHUMAYLOV, Z., KAZHDAN, D., ZHAO, Y., PAPERNOT, N., ERDOGDU, M. A., AND ANDERSON, R. J. Manipulating SGD with data ordering attacks. In *Advances in Neural Information Processing Systems 34: Annual Conference on Neural Information Processing Systems 2021, NeurIPS 2021, December 6-14, 2021, virtual* (2021), M. Ranzato, A. Beygelzimer, Y. N. Dauphin, P. Liang, and J. W. Vaughan, Eds., pp. 18021–18032.

[49] STERN, M., SHAZEE, N., AND USZKOREIT, J. Block-wise parallel decoding for deep autoregressive models. In *Advances in Neural Information Processing Systems 31: Annual Conference on Neural Information Processing Systems 2018, NeurIPS 2018, December 3-8, 2018, Montréal, Canada* (2018), S. Bengio, H. M. Wallach, H. Larochelle, K. Grauman, N. Cesa-Bianchi, and R. Garnett, Eds., pp. 10107–10116.

[50] SUN, S., LI, Y., LI, X., LIAN, Y., LIN, W., ZHEN, H., YANG, Z., CHEN, C., YU, X., YUAN, M., AND MA, C. Scaling up, speeding up: A benchmark of speculative decoding for efficient LLM test-time scaling. *CoRR abs/2509.04474* (2025).

[51] TANG, Y., GUO, Z. D., ZHENG, Z., CALANDRIELLO, D., CAO, Y., TARASSOV, E., MUNOS, R., PIRES, B. Á., VALKO, M., CHENG, Y., AND DABNEY, W. Understanding the performance gap between online and offline alignment algorithms. *CoRR abs/2405.08448* (2024).

[52] TEAM, K., DU, A., GAO, B., AND ET.AL. Kimi k1.5: Scaling reinforcement learning with llms. *CoRR abs/2501.12599* (2025).

[53] TEAM, Q. Qwen2.5: A party of foundation models, September 2024.

[54] WEI, X., HUANG, Z., SUN, T., HAO, Y., CHEN, R., HAN, M., GU, J., AND CHEN, H. Phoenixos: Concurrent os-level GPU checkpoint and restore with validated speculation. In *Proceedings of the ACM SIGOPS 31st Symposium on Operating Systems Principles, SOSP 2025, Lotte Hotel World, Seoul, Republic of Korea, October 13-16, 2025* (2025), Y. Won, Y. Kwon, D. Yuan, and R. Isaacs, Eds., ACM, pp. 996–1013.

[55] WU, B., LIU, S., ZHONG, Y., SUN, P., LIU, X., AND JIN, X. Loongserve: Efficiently serving long-context large language models with elastic sequence parallelism. In *Proceedings of the ACM SIGOPS 30th Symposium on Operating Systems Principles, SOSP 2024, Austin, TX, USA, November 4-6, 2024* (2024), E. Witchel, C. J. Rossbach, A. C. Arpaci-Dusseau, and K. Keeton, Eds., ACM, pp. 640–654.

[56] WU, D. X., YUN, C., AND SRA, S. On the training instability of shuffling SGD with batch normalization. In *International Conference on Machine Learning, ICML 2023, 23-29 July 2023, Honolulu, Hawaii, USA* (2023), A. Krause, E. Brunskill, K. Cho, B. Engelhardt, S. Sabato, and J. Scarlett, Eds., vol. 202 of *Proceedings of Machine Learning Research*, PMLR, pp. 37787–37845.

[57] XIA, H., YANG, Z., DONG, Q., WANG, P., LI, Y., GE, T., LIU, T., LI, W., AND SUI, Z. Unlocking efficiency in large language model inference: A comprehensive survey of speculative decoding. In *Findings of the Association for Computational Linguistics, ACL 2024, Bangkok, Thailand and virtual meeting, August 11-16, 2024* (2024), L. Ku, A. Martins, and V. Srikumar, Eds., Association for Computational Linguistics, pp. 7655–7671.

[58] XIANG, Y., LI, X., QIAN, K., YANG, Y., ZHU, D., YU, W., ZHAI, E., LIU, X., JIN, X., AND ZHOU, J. Aegaon: Effective GPU pooling for concurrent LLM serving on the market. In *Proceedings of the ACM SIGOPS 31st Symposium on Operating Systems Principles, SOSP 2025, Lotte Hotel World, Seoul, Republic of Korea, October 13-16, 2025* (2025), Y. Won, Y. Kwon, D. Yuan, and R. Isaacs, Eds., ACM, pp. 1030–1045.

[59] YAO, J., CHENG, R., WU, X., WU, J., AND TAN, K. C. Diversity-aware policy optimization for large language model reasoning. *CoRR abs/2505.23433* (2025).

[60] YAO, Z., GHOLAMI, A., LEI, Q., KEUTZER, K., AND MACHONEY, M. W. Hessian-based analysis of large batch training and robustness to adversaries. In *Advances in Neural Information Processing Systems 31: Annual Conference on Neural Information Processing Systems 2018, NeurIPS 2018, December 3-8, 2018, Montréal, Canada* (2018), S. Bengio, H. M. Wallach, H. Larochelle, K. Grauman, N. Cesa-Bianchi, and R. Garnett, Eds., pp. 4954–4964.

[61] YU, Q., ZHANG, Z., ZHU, R., YUAN, Y., ZUO, X., YUE, Y., FAN, T., LIU, G., LIU, L., LIU, X., LIN, H., LIN, Z., MA, B., SHENG, G., TONG, Y., ZHANG, C., ZHANG, M., ZHANG, W., ZHU, H., ZHU, J., CHEN, J., CHEN, J., WANG, C., YU, H., DAI, W., SONG, Y., WEI, X., ZHOU, H., LIU, J., MA, W., ZHANG, Y., YAN, L., QIAO, M., WU, Y., AND WANG, M. DAPO: an open-source LLM reinforcement learning system at scale. *CoRR abs/2503.14476* (2025).

[62] YUE, Y., YUAN, Y., YU, Q., ZUO, X., ZHU, R., XU, W., CHEN, J., WANG, C., FAN, T., DU, Z., WEI, X., YU, X., LIU, G., LIU, J., LIU, L., LIN, H., LIN, Z., MA, B., ZHANG, C., ZHANG, M., ZHANG, W., ZHU, H., ZHANG, R., LIU, X., WANG, M., WU, Y., AND YAN, L. VAPO: efficient and reliable reinforcement learning for advanced reasoning tasks. *CoRR abs/2504.05118* (2025).

[63] ZAN, D., HUANG, Z., LIU, W., CHEN, H., ZHANG, L., XIN, S., CHEN, L., LIU, Q., ZHONG, X., LI, A., LIU, S., XIAO, Y., CHEN, L., ZHANG, Y., SU, J., LIU, T., LONG, R., SHEN, K., AND XIANG, L. Multi-swe-bench: A multilingual benchmark for issue resolving. *CoRR abs/2504.02605* (2025).

[64] ZENG, S., XIE, M., GAO, S., CHEN, Y., AND LU, Y. Medusa: Accelerating serverless LLM inference with materialization. In *Proceedings of the 30th ACM International Conference on Architectural Support for Programming Languages and Operating Systems, Volume 1, ASPLOS 2025, Rotterdam, The Netherlands, 30 March 2025 - 3 April 2025* (2025), L. Eeckhout, G. Smaragdakis, K. Liang, A. Sampson, M. A. Kim, and C. J. Rossbach, Eds., ACM, pp. 653–668.

[65] ZHANG, D., WANG, H., LIU, Y., WEI, X., SHAN, Y., CHEN, R., AND CHEN, H. Blitzscale: Fast and live model autoscaling with O(1) host caching. In *19th USENIX Symposium on Operating Systems Design and Implementation, OSDI 2025, Boston, MA, USA, July 7-9, 2025* (2025), L. Zhou and Y. Zhou, Eds., USENIX Association, pp. 275–293.

[66] ZHANG, G., GENG, H., YU, X., YIN, Z., ZHANG, Z., TAN, Z., ZHOU, H., LI, Z., XUE, X., LI, Y., ZHOU, Y., CHEN, Y., ZHANG, C., FAN, Y., WANG, Z., HUANG, S., LIAO, Y., WANG, H., YANG, M., JI, H., LITTMAN, M., WANG, J., YAN, S., TORR, P., AND BAI, L. The landscape of agentic reinforcement learning for llms: A survey. *CoRR abs/2509.02547* (2025).

[67] ZHANG, Z., JIANG, Z., JIANG, C., YU, M., ZHENG, S., LIN, H., HOFFMANN, H., AND LIU, X. Swiftspec: Ultra-low latency LLM decoding by scaling asynchronous speculative decoding. *CoRR abs/2506.11309* (2025).

[68] ZHENG, C., LIU, S., LI, M., CHEN, X.-H., YU, B., GAO, C., DANG, K., LIU, Y., MEN, R., YANG, A., ZHOU, J., AND LIN, J. Group sequence policy optimization, 2025.

[69] ZHONG, Y., ZHANG, Z., SONG, X., HU, H., JIN, C., WU, B., CHEN, N., CHEN, Y., ZHOU, Y., WAN, C., ZHOU, H., JIANG, Y., ZHU, Y., AND JIANG, D. Streamrl: Scalable, heterogeneous, and elastic RL for llms with disaggregated stream generation. *CoRR abs/2504.15930* (2025).

[70] ZHONG, Y., ZHANG, Z., WU, B., LIU, S., CHEN, Y., WAN, C., HU, H., XIA, L., MING, R., ZHU, Y., AND JIN, X. Rlh-fuse: Efficient RLHF training for large language models with inter- and intra-stage fusion. *CoRR abs/2409.13221* (2024).

[71] ZHONG, Y., ZHANG, Z., WU, B., LIU, S., CHEN, Y., WAN, C., HU, H., XIA, L., MING, R., ZHU, Y., AND JIN, X. Optimizing RLHF training for large language models with stage fusion. In *22nd USENIX Symposium on Networked Systems Design and Implementation, NSDI 2025, Philadelphia, PA, USA, April 28-30, 2025* (2025), T. A. Benson and R. N. Mysore, Eds., USENIX Association, pp. 489–503.

[72] ZHU, K., GAO, Y., ZHAO, Y., ZHAO, L., ZUO, G., GU, Y., XIE, D., YE, Z., KAMAHORI, K., LIN, C., WANG, Z., WANG, S., KRISHNAMURTHY, A., AND KASIKCI, B. Nanoflow: Towards optimal large language model serving throughput. In *19th USENIX Symposium on Operating Systems Design and Implementation, OSDI 2025, Boston, MA, USA, July 7-9, 2025* (2025), L. Zhou and Y. Zhou, Eds., USENIX Association, pp. 749–765.